Physico-chemical Studies on Surface Active Agents. (VI)

The Formation of Positive Silver Iodide Sols in the Presence of Anionic Surface Active Agents

Akira WATANABE*

(Tachi Laboratory)

The kinetics of formation of positive silver iodide sols in the presence of anionic surface active agents, *i.e.* alkyl sulphates, sulphonates and an alkyl phosphate, have been studied by measuring the turbidity change with time. It was found that the effect of these substances on sol formation showed marked similarity to their effect on formed sols described in Part 2. Over certain concentration range of the surface active agent, coagulation of the sol particles formed occurred and at higher concentrations sensitisation was found to have taken place. It was proved by ζ potential measurements that the coagulation was due to the change in the Stern potential. The overall reaction mechanism was the simultaneous occurrence of crystal growth and coagulation, both of which were influenced by the change in the particle charge due to the adsorption of the surface active agents. An attempt was made to give a semi-quantitative treatment of the reaction mechanism.

I. INTRODUCTION

One of the useful methods of studying the effect of surface active agents on hydrophobic sols is to examine the influence of the presence of these substances on sol formation. It was found by Matijević and Ottewill[1,2] that under certain conditions the presence of cationic surface active agents had a strong influence on the formation of negative silver iodide sols and that this phenomenon was intimately related to the change in surface potential of the sol particles formed. It was also shown by electron microscopy that the large [change in turbidity with time during the formation was due to the coagulation of these particles.

In this paper the results of experiments made on positive silver iodide sols, using the same anionic surface active agents as those used in the coagulation study on *formed* sols (Part 2[3]) are described. Comparison of the results with those obtained in Part 2 shows an intimate relationship between them, thus suggesting the occurrence of coagulation (and sensitisation) in certain concentration ranges of surface active agents.

The mechanism of the overall reaction is complicated by the fact that the particle growth occurs simultaneously with coagulation in certain concentration ranges. However, an attempt has been made to give a qualitative explanation of the reaction behaviour, using the concepts developed in Part 5[4].

* 渡 辺　　昌

II. EXPERIMENTAL

1. Materials

The anionic surface active agents and other materials used were the same as those described in Part 2[3].

2. Methods of Measurements

(i) Turbidity

Aliquots of a silver nitrate stock solution were mixed with different amounts of surface active agent stock solutions and then diluted to 10 ml with redistilled water. In this way solutions were obtained which contained silver nitrate at a constant concentration and the surface active agent at concentrations varying systematically. 0.1 ml of $3 \times 10^{-2} M$ potassium iodide stock solution was added to 3 ml of the above solution in the optical cell by means of the mixer. The turbidity change with time after mixing was followed by the same method as described in Part 2. The concentration of silver nitrate was so chosen that the final sol concentration was $10^{-3} M$ with a pAg value of 3. Since the final sol contained also $10^{-3} M$ potassium nitrate, the final ionic strength of the sol was $2 \times 10^{-3} M$.

(ii) Microelectrophoresis

In order to determine changes of particle charge a series of measurements was made on silver iodide sol particles formed in the presence of SDS.

A 1 ml of $10^{-2} M$ potassium iodide solution was added with vigorous shaking to 9 ml of solution in a Pyrex test tube; these solutions contained silver nitrate at constant concentration and SDS at concentrations which varied systematically. The method of preparing these solutions was the same as that used in the last section. The concentration of silver nitrate was so chosen that the final sol concentration, pAg and ionic strength were the same as those in the turbidity measurements.

The mobility measurements were made by the method employed in Part 2 and were started 15 min after formation of the sols.

(iii) Electron Micrographs

These were obtained by the methods previously described[3].

III. RESULTS

1. Turbidity Measurements

(i) Optical Density *vs.* Time Curves

The changes in turbidity with time which occurred after mixing the silver nitrate solutions with potassium iodide were strongly influenced by the presence of surface active agents. In Fig. 1 and 2 the Δ optical density *vs.* time curves for alkyl sulphates and sulphonates are given. It is clear that these curves have shapes similar to the coagulation curves in Part 2 and in the coagulation range the early stages of the curves are usually sufficiently linear to enable accurate values of $(dt/dD)_{t \to 0}$ to be obtained.

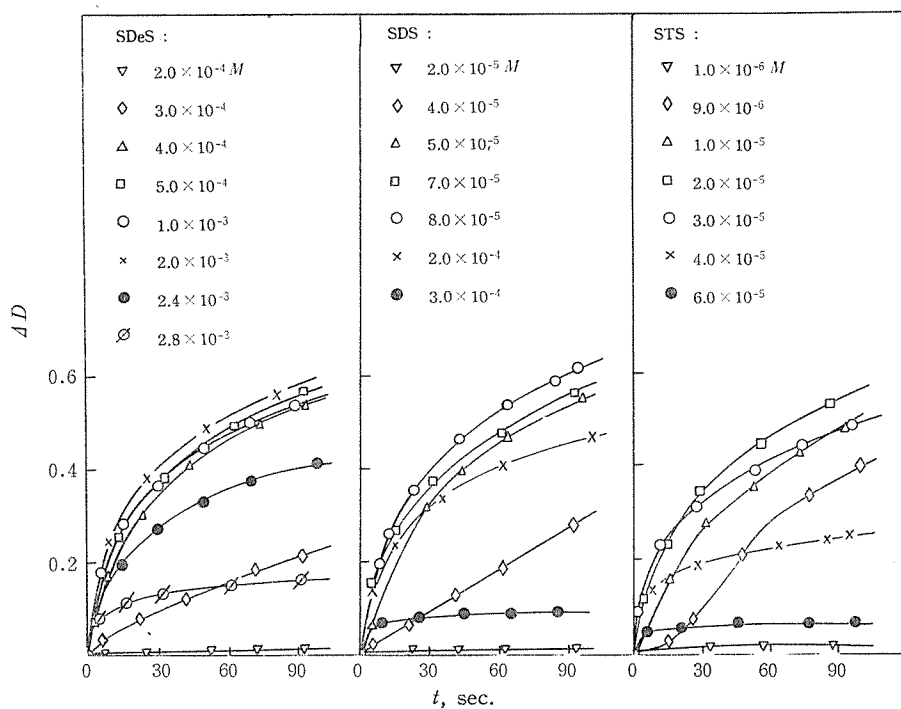In many cases, especially at low concentrations of surface active agent, "sigmoid

Fig. 1. $\varDelta$ Optical density *vs.* time for formation of Ag I sols in the presence of alkyl sulphates. AgNO$_3$: $2\times10^{-3}M$, KI: $10^{-3}M$.
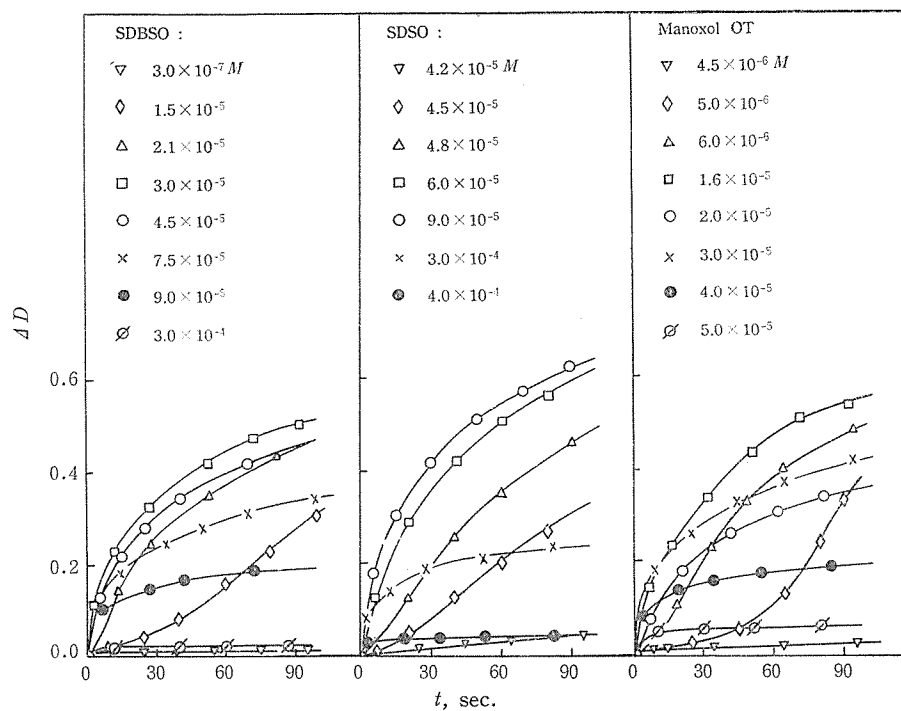

Fig. 2. $\varDelta$ Optical density *vs.* time for formation of Ag I sols in the presence of surface active sulphonates. AgNO$_3$: $2\times10^{-3}M$, KI: $10^{-3}M$.

·curves" were obtained. It will be shown later in this paper that the first portion of the curve corresponds to crystal growth and that the rapid increase of optical ·density in the later stages is due to slow coagulation, see *e. g*. Fig. 9.

(ii) Optical Density at Different Times

In order to observe the general aspects of the influence of various anionic surface active agents on the formation of positive silver iodide sols, the method of plotting adopted in Part 2 was used, *vide* Fig. 12 of Part 2. The curves for SDS are given in Fig. 3. It is clear that the turbidity change is very marked over a ·certain concentration range of the surface active agent.
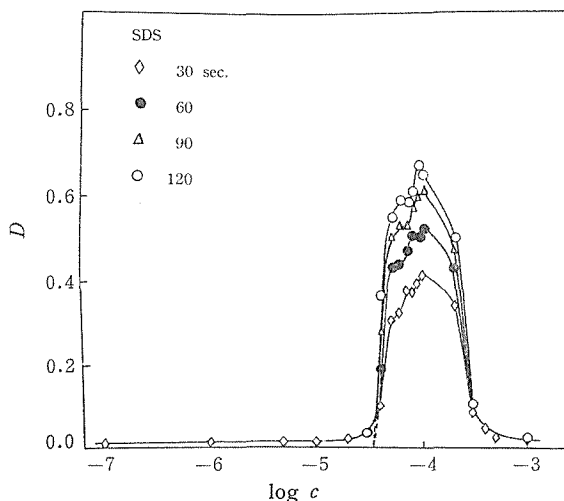

Fig. 3. Formation of Ag I sol in the presence of SDS.
AgNO$_3$: $2 \times 10^{-3} M$, KI: $1 \times 10^{-3} M$.

It has been found by electron microscopy that coagulation is taking place in this concentration range, *vide* section 3. Hence, by analogy with the case of co-agulation of *formed* sols of Part 2 we can determine the "coagulation concentration" for the, so called, *nascent* state by extrapolating the steeply rising portion of the curves to the log *c* axis, *cf*. Part 2. It has been found that the extrapolation of ·curves for different times after mixing usually gives the same coagulation concen-tration for a given surface active agent. In Table 1 are given the values thus obtained together with the coagulation concentration for *formed* sols listed in Table 2 of Part 2. Comparison of these two sets of values shows a marked relationship between them; for increasing coagulation concentrations both give the same se-quence of surface active agents. However, the coagulation concentrations for *nascent* sols are always slightly higher than those for *formed* sols; this can possibly be explained by the smaller particle size, see Discussion.

(iii) Effect of Chain Length

The optical densities 90 sec after mixing were plotted against the logarithm of the concentration of alkyl sulphates and sulphonates in Fig. 4 and 5, respectively. It is clear that the concentration range, in which coagulation occurs, is lower for the longer chain. A direct comparison of the curves with those in Fig. 13 and 14 of
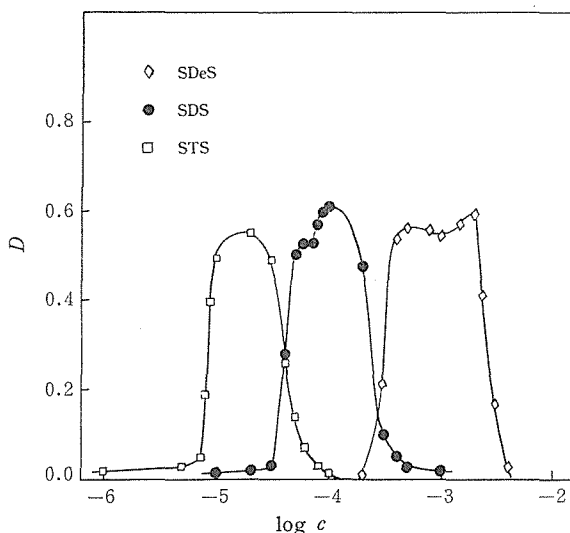
Fig. 4. Formation of Ag I sol in the presence of alkyl sulphates. Optical densities, 90 sec. after mixing.
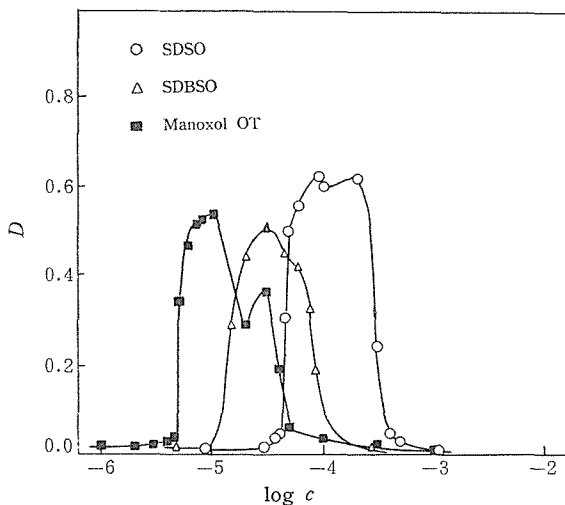

Fig. 5. Formation of Ag I sols in the presence of surface active sulphonates. Optical densities, 90 sec. after mixing.

Part 2 shows that the coagulation range is generally wider in the present case than for the corresponding range in the case of *formed* sols.

At higher concentrations of Manoxol OT another peak is found, which was not present in the case of the *formed* sol. The same phenomenon has already been described by Matijević and Ottewill[1] in the formation of negative sols in the presence of cationic surface active agents, and has been related to the zig-zag change of ζ potential of the particles with increasing surface active agent concentrations. The same explanation may also be applicable in the present case.

(iv) **Effect of Head Group Size**

The optical densities (90 sec after mixing) were plotted against the log c for

SDS, SDSO and DHP in Fig. 6. The curves are almost superposed, indicating that the coagulation concentration range is almost independent of the head group size, although it is strongly dependent on chain length.
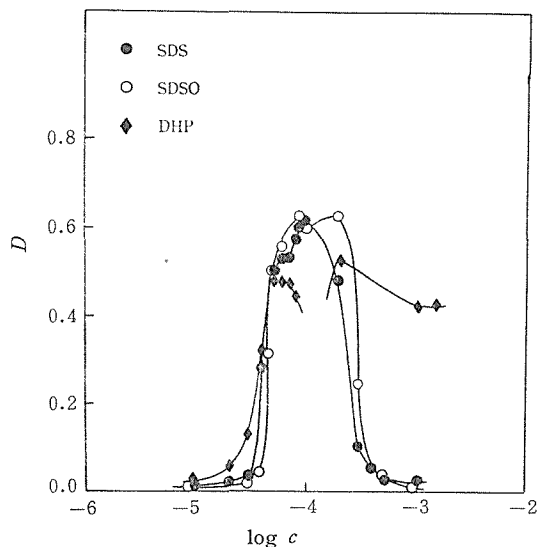

Fig. 6. Formation of Ag I sols in the presence of dodecyl sulphate, sulphonate and phosphate. Optical densities, 90 sec. after mixing.

(v) Anomalous Behaviour with DHP

The optical density becomes high at higher concentrations of DHP, an anomaly which has been shown to be due to the formation of the insoluble silver salt of the DP$^-$ ion in this region. In Fig. 7 are shown the curves of Δ optical density $vs.$ log c of DHP, at times of 30, 60, 90 and 120 sec after mixing aliquots of DHP solutions
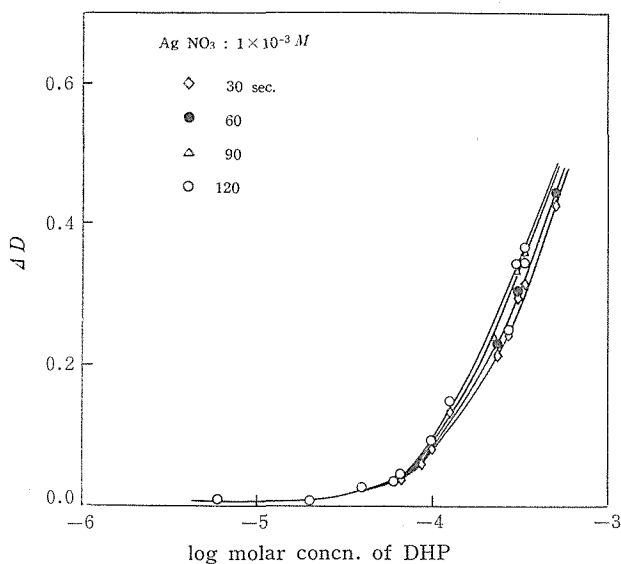

Fig. 7. Formation of silver dodecyl phosphate.

Table 1. Coagulation of positive silver iodide sols by
anionic surface active agents.

Surface active agent	Coagulation concentration M	
	Nascent sol	*Formed* sol
SDeS	2.80×10^{-4}	2.46×10^{-4}
SDS	3.55×10^{-5}	1.29×10^{-5}
STS	7.95×10^{-6}	3.98×10^{-6}
SDSO	4.72×10^{-5}	3.24×10^{-5}
SDBSO	1.27×10^{-5}	6.92×10^{-6}
Manoxol OT	4.79×10^{-6}	3.24×10^{-6}
DHP	2.95×10^{-5}	4.91×10^{-6}

with 3 ml of $10^{-3} M$ silver nitrate solution in the optical cell. It is clear from these curves that at concentrations of DHP higher than *ca.* $10^{-4} M$ the optical density change due to formation of the insoluble silver salt of DHP is comparable to that due to coagulation of the silver iodide sol, but at concentrations of DHP lower than this, the optical density change obtained is almost completely due to the latter process. Hence, the first peak of the curve in Fig. 6 is comparable to those for the other surface active agents.

At concentrations of DHP higher than $10^{-4} M$, the DHP in the initial solution before mixing will probably be in the form of insoluble Ag(DP), since enough silver ion is present for salt formation to occur; as the *p*H of the DHP solution used was *ca.* 4.5, the singly ionized form of DHP would be predominant, see Part 2. In fact, the initial optical density of the solution in the optical cell was as high as *ca.* 0.2 in these experiments. Immediately after mixing with potassium iodide solution, the optical density fell to the more usual value for silver iodide sols. This can be explained by double decomposition taking place according to the equation

$$Ag(DP) + KI = Ag I + K(DP).$$
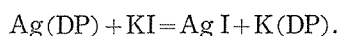
The solubility of K(DP) is high and therefore this material does not contribute to the optical density of the sol. As the particle size of the silver iodide sol thus formed is small, the optical density drops from the initial value, due to the insoluble Ag(DP) salt, to the normal value for the silver iodide sol.

After this instantaneous drop, the optical density increases gradually and the usual type of curve for silver iodide sol formation in the presence of surface active agent is obtained.

2. Mobility Measurements

Strictly speaking, the mobility of the silver iodide sol particles in the initial reaction mixture may not have the same value as that measured 15 min after initiation. Since it is experimentally very difficult to carry out mobility measurements during the initial reaction, a series of measurements has been made on particles 15 min after mixing in order to obtain some idea about the surface charge of the particles.

Although it took approximately 20 to 30 min to complete one run at each con-

centration of SDS, the mobility appeared to remain practically constant over the whole of this period, at concentrations of SDS either lower than *ca.* $10^{-5} M$ or higher than the zero point of ζ. In the intermediate concentration range, however, the mobility increased gradually with time and then tended to a constant value. The final value has been chosen in the present case for the sake of practical convenience. Although it may be more reasonable to use the initial mobility value, it was not possible in practice, since at least twenty readings were necessary in order to obtain an average value.

The ζ *vs.* log *c* curve for SDS thus obtained is given in Fig. 8. In the same figure the curve for a *formed* sol in Part 2 has been plotted in order to show the difference between them. Both the relaxation and Henry corrections were applied in calculating the values of ζ from mobility data. The particle radius was taken to be 10^{-6} cm. Although this is rather an approximation, it makes little difference to the discussion of the essential features of the ζ potential behaviour.
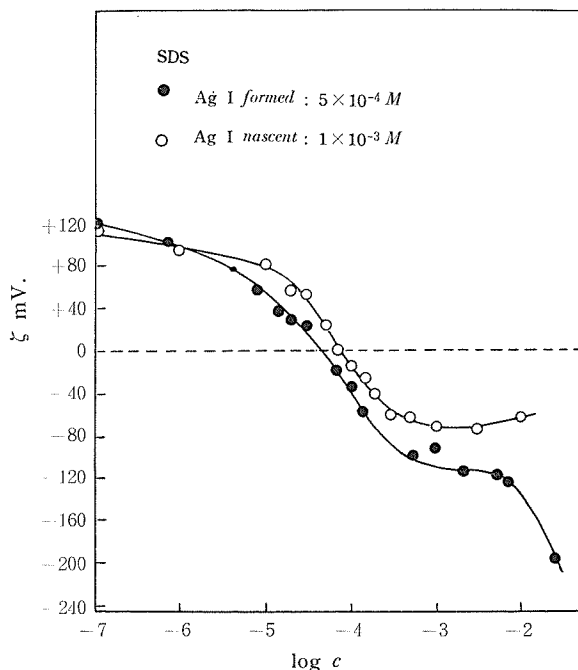

SDS

● Ag I *formed* : $5 \times 10^{-4} M$

○ Ag I *nascent* : $1 \times 10^{-3} M$

Fig. 8. ζ *vs.* log molar concn. of SDS

The general shape of the curve is almost the same as in the case of *formed* sols but reversal of charge occurs at a slightly higher surface active agent concentration. Although in the case of *formed* sols a rapid increase of ζ potential in the negative direction was found near the c. m. c., such behaviour was not observed in the present case. In the case of *formed* sols interaction with micelles appeared to occur leading to mutual coagulation; thus binding the micelles to the particles gives a large increase in mobility. When sols are formed in the presence of surface active agents, however, crystal growth appears to be inhibited to a large extent, *vide* Part 5; the nuclei formed are coated with surface active agents which acts as

a barrier to ion deposition. Thus, in the latter case the particles are coated with an adsorbed layer of SDS (high negative charge) from the early stages of formation, thus the possibility of interaction with micelles did not occur. This is also confirmed from the optical density against time curves inasmuch as that a second coagulation region did not occur in the neighbourhood of the c. m. c.
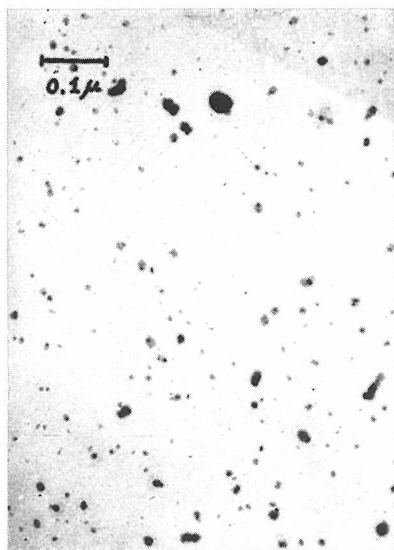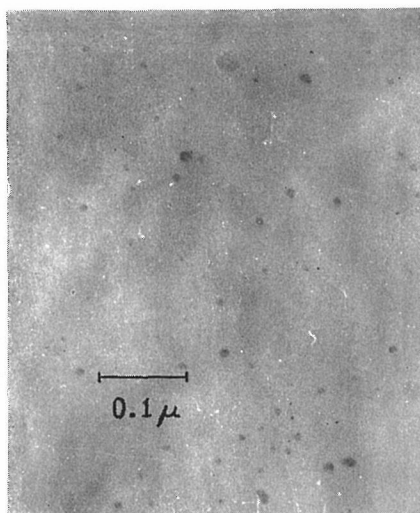

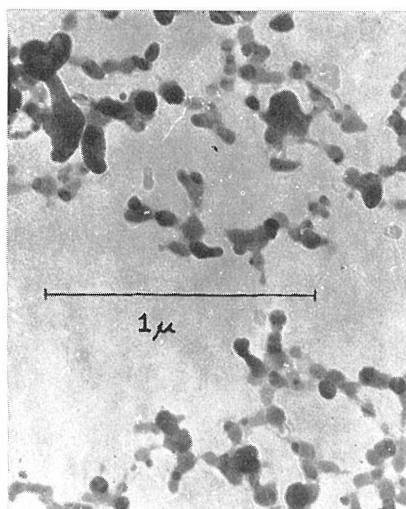(A$_1$) SDS, $5 \times 10^{-6} M$

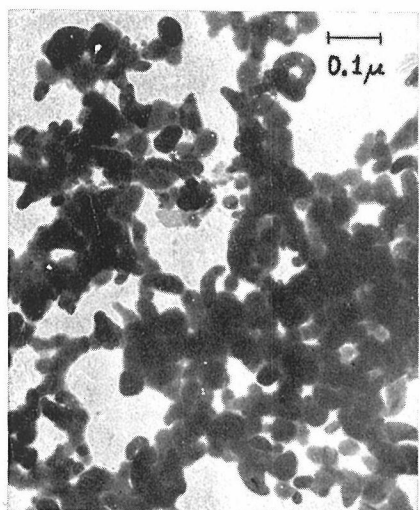(A$_2$) SDS, $7 \times 10^{-5} M$
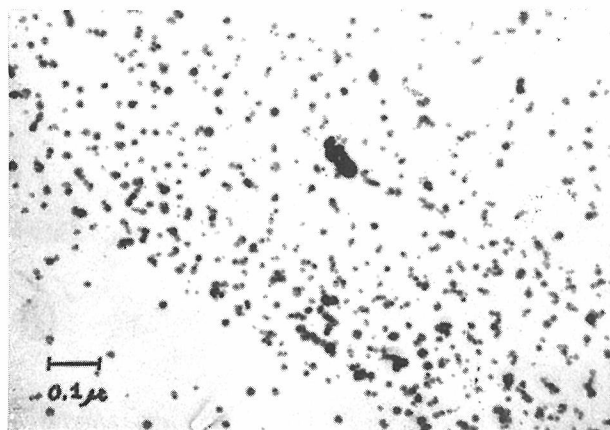
(A$_3$) SDS, $7 \times 10^{-4} M$

Fig. 9. Electron micrographs of positive silver iodide sol particles formed in the presence of surface active agents.
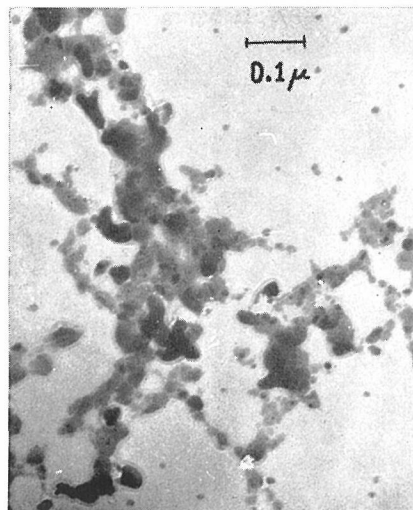
(B₁) Manoxol OT, $10^{-6} M$

(B₂) Manoxol OT, $8 \times 10^{-6} M$

(B₃) Manoxol OT, $2 \times 10^{-5} M$

(B₄) Manoxol OT, $10^{-4} M$

Fig. 9. Electron micrographs of positive silver iodide sol particles
formed in the presence of surface active agents.

(B$_5$) Manoxol OT, $5 \times 10^{-6} M$; 10 sec after mixing.

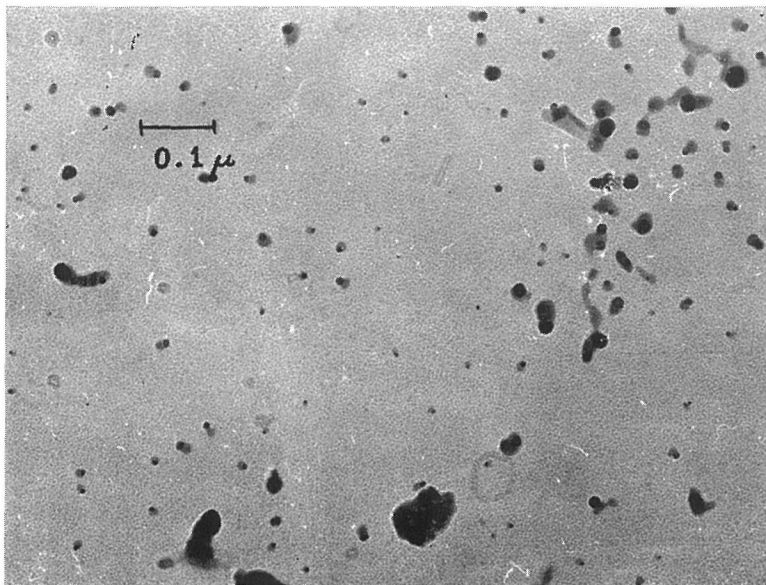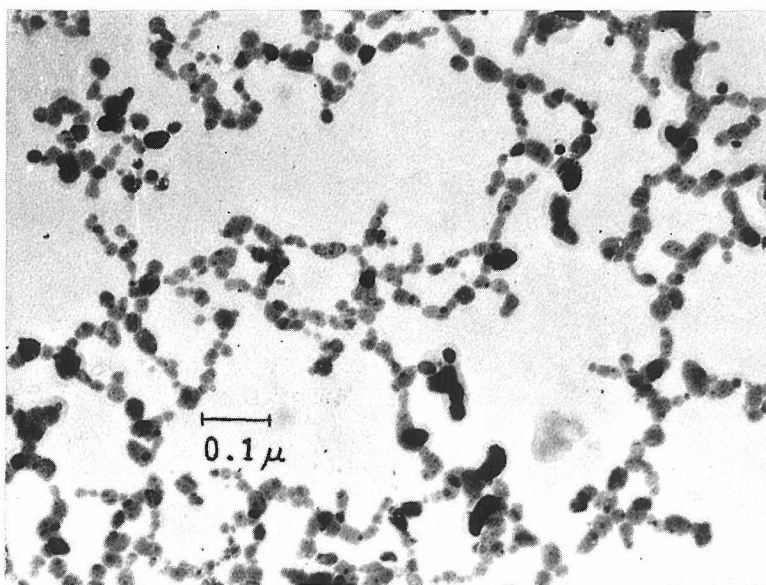(B$_6$) Manoxol OT, $5 \times 10^{-6} M$; 70 sec after mixing.

Fig. 9. Electron micrographs of positive silver iodide sol particles formed in the presence of surface active agents.

3. Electron Micrographs

In Fig. 9 the electron micrographs of the silver iodide sol particles formed in the presence of SDS and Manoxol OT are given. These were taken in order to obtain some idea of the manner in which coagulation was taking place.

The set of micrographs (A) are for SDS at different concentrations. (A_1) is for a concentration lower than the coagulation range, $i.\,e.$ $5 \times 10^{-6}\,M$, (A_2) for a concentration corresponding to the maximum of the coagulation curve, $i.\,e.$ $7 \times 10^{-5}\,M$, and (A_3) for a concentration in the protected range, $i.\,e.$ $7 \times 10^{-4}\,M$. These micrographs show clearly the occurrence of coagulation at a concentration corresponding to that obtained from the turbidity measurements, $cf.$ Fig. 4.

The set of micrographs (B) are for Manoxol OT. (B_1) is for a concentration lower than the coagulation range, $i.\,e.$ $10^{-6}\,M$, (B_2) and (B_3) are for concentrations in the coagulation range, $i.\,e.$ 8×10^{-6} and $2 \times 10^{-5}\,M$, and (B_4) is for a concentration in the protected range, $i.\,e.$ $10^{-4}\,M$, $cf.$ Fig. 5. It was observed that the degree of coagulation was much smaller at the concentration of $10^{-4}\,M$, than expected from the turbidy data, and it is interesting to note that the coagula are linear networks in this case. This appears to suggest that the adsorption of Manoxol OT is taking place mainly on certain crystal faces.

(B_5) and (B_6) are for the same concentration of Manoxol OT, $i.\,e.$ $5 \times 10^{-6}\,M$, but for different times, $i.\,e.$ 10 and 70 sec, after mixing. At this concentration, the optical density $vs.$ time curve is sigmoid, $cf.$ Fig. 2. It is observed that little coagulation is taking place in the initial stages of the reaction, but at the later stage dense networks are formed due to coagulation.

IV. DISCUSSION

1. Adsorption Behaviour of Surface Active Agents

It is clear from equation (15) of Part 2 that the gradient of the ζ $vs.$ log c curve at the zero point of ζ is a function of the ζ potential of the original surface, the ionic strength, the particle radius and the number of adsorption sites per unit area; whereas, the concentration of surface active agent at which $\zeta = 0$ is also dependent on the adsorption constant k_2, see equation (16) of Part 2. The fact that both curves in Fig. 8 are very nearly parallel at $\zeta = 0$ suggests that at the time of the electrophoresis measurements the conditions of the two sols were very similar, thus indicating that the assumption of $a = 100\,\text{Å}$ for particle radius was probably a very reasonable one.

There is, on the other hand, a slight difference in the zero point of ζ for the two cases. It is clear from equation (16) of Part 2 that the larger the value of τ, the larger will be the value of c^0, if all of the other quantities are the same; ζ^* is defined by the pAg of the sol, and N_1 and k_2 are related to the properties of the surface active agents and the silver iodide surface, both being the same for the $nascent$ and the $formed$ sols. However, the values of τ are 1.41 for the former and 1.23 for the latter. It can, therefore, be expected that the value of c^0 will be larger for the $nascent$ sol; this has actually been observed in Fig. 8.

2. Reaction Mechanism of the Whole Process

The reactions occurring in the present system can be considered in a similar manner to those described in the last paper; it is also complicated by the fact that the overall reaction is a consecutive or simultaneous combination of various processes, *viz.* nucleation, crystal growth and coagulation or sensitisation. However, the problem is a little simpler than the case treated in the last paper, since the concentrations of the reactants, *i. e.* silver and iodide ions, are kept constant and at a condition of high supersaturation. Moreover, the concentration of the added surface active agents is usually very small and hence no change in ionic strength occurs. In this sense, the present problem can be considered as a special case of the general problem discussed in Part 5.

(i) Nucleation

a. Nucleation rate. It is clear that, in equations (1) and (3) of Part 5 the only quantities which might change by addition of surface active agent are A_1 and W_n. However, this change will be very small or practically zero. Firstly, it seems very unlikely that a surface active agent with a large head group will be adsorbed on to such a small cluster of molecules as a nucleus. Moreover, the solubilities of the silver salts of the surface active agents used are fairly high, suggesting that the bond strength between the silver ion and the head groups is not large. Hence, such binding will probably not take place in the concentration range of major interest until the particle grows to a certain size of macroscopic order. Here the term "macroscopic" order means an initial size at which the hydrophobic character of the alkyl chain becomes effective in causing adsorption on to the particle surface.

Secondly, even if a change in interfacial free energy occurs due to a decrease in surface charge density, *i. e.* electrocapillarity, this would be negligible compared with the intrinsic value of the interfacial free energy, see Appendix of Part 5.

These considerations suggest that, as long as the system is restricted to silver iodide sol formation at constant concentrations of the reactants, the nucleation rate will be the same even if additional surface active agents are present in the system.

It is to be expected that at the high supersaturations used in the present case, *i. e.* $10^{-3} M$ Ag I, the nucleation rate will be rapid and will not influence the net rate of the whole process.

b. Induction time. Equation (4) of Part 5 shows that the induction time decreases very rapidly with increasing supersaturation. Hence, it is to be expected that the induction time of nucleation will be practically zero in the present case.

(ii) Crystal Growth

a. The effect of surface charge on growth rate. If it is assumed that the mechanism of crystal growth of silver iodide is the alternate deposition of the silver and iodide ions on the surface, the growth rate will be determined by the slower step among these two depositions. This means that in the case of positively charged particles the growth rate is retarded by the slow deposition of silver ions and for negatively charged particles it is retarded by the slow deposition of iodide ions.

This retardation can be attributed to two mechanisms, namely increase in potential barrier, equation (6) of Part 5, and deficit of the reactant at the surface, equation (7) of Part 5, both occurring by virtue of the increase in the absolute value of ψ_δ.

b. Growth equation. For a spherical particle of radius a, volume V_S, surface area S and density d, the following equations hold,

$$S = 4\pi a^2, \quad V_S = (4/3)\pi a^3 \text{ and } m = V_S d \tag{1}$$

Hence, equation (5) of Part 5 becomes

$$d V_S/dt = k'' V_S^{2/3}(c_i - c_i^s) \tag{2}$$

where

$$k'' = (36\pi)^{1/3} k/d \tag{3}$$

The solution of equation (2) is given by

$$3 V_S^{1/3} = k'' \int_0^t (c_i - c_i^s)\, dt + 3 V_0^{1/3} \tag{4}$$

where V_0 is the volume of the particle at $t = 0$.

In order to obtain a more explicit formula for V as a function of t, it is necessary to obtain the functional relation between c_i and t; this has been derived by various authors[5,6,7]. However, the solution obtained is rather complicated, and, as we are primarily interested in the initial stage of the process, the assumption will be made that for this stage the change in c_i is small compared with the supersaturation, $(c_i - c_i^s)$. That is, $(c_i - c_i^s)$ remains practically constant with time. Making this assumption equation (4) reads

$$V_S = V_0 [1 + (k''/3 V_0^{1/3})(c_i - c_i^s)\, t]^3 \tag{5}$$

$$\cong V_0 [1 + (k''/V_0^{1/3})(c_i - c_i^s)\, t] \tag{5A}$$

and

$$a = a_0 [1 + (k''/3 V_0^{1/3})(c_i - c_i^s)\, t] \tag{6}$$

where a_0 is the initial particle radius at $t = 0$.

(iii) Coagulation

It was shown that the ζ potential *vs.* log c curves in the presence of surface active agents showed the same behaviour as in the case of formed sols. This suggests that the coagulation probably takes place due to the decrease in surface potential near the zero point of ζ. If this is the case, the coagulation concentrations in Table 1 for the *nascent* sols will be closely related to the zero point of ζ. Comparison of the curves in Fig. 13, 14 and 15 of Part 2 with those in Fig. 4, 5 and 6 of this paper shows that, as expected from the shift of the zero point of ζ explained in section 1, the coagulation ranges are always shifted towards higher surface active agent concentrations in the cases of sol formation.

(iv) The Turbidity Change for the Whole Reaction

In the early stages of the coagulation process, the turbidity of a sol is related to the volume and the number of particles by equation (4) of Part 2.

For the coagulation of a *formed* sol, this suggests a linear relationship between

τ' and t; this has been proved experimentally for most concentrations of surface active agents in the coagulation range, see Part 2. However, this does not always hold in the present case, because the size of the primary particles V_s, and hence their radius a, are functions of time; the number of particles, N_b, will probably be practically constant because of the rapid nucleation, see section (i).

Therefore substituting V_s and a from equations (5 A) and (6) in equation (4) of Part 2, we obtain

$$\tau' = A_R V_0^2 N_b \left\{ 1 + \frac{k''}{V_0^{1/3}} (c_l - c_l^s) \, t \right\}^2$$

$$\times \left[1 + \frac{16 \pi \, \mathcal{D} \, N_b \, a_0}{W} \left\{ 1 + \frac{k''}{3 \, V_0^{1/3}} (c_l - c_l^s) \, t \right\} t \right]$$

$$= A_R V_0^2 N_b \left[1 + \frac{2 \, k''}{V_0^{1/3}} \left\{ (c_l - c_l^s) + \frac{8 \pi \, \mathcal{D} \, N_b \, a_0}{W} \right\} t \right.$$

$$+ \frac{k''}{V_0^{1/3}} (c_l - c_l^s) \left\{ \frac{k''}{V_0^{1/3}} (c_l - c_l^s) + \frac{112 \pi \, \mathcal{D} \, N_b \, a_0}{W} \right\} t^2 + o \, (t^3) \qquad (7)$$

This gives the initial change of turbidity with time when the particle growth is taking place in a coagulation process.

This equation can be simplfied for special cases; for $1/W \ll k''(c_l - c_l^s)$, at low surface active agent concentrations where the stability of the sol formed is high,

$$\tau' = A_R V_0^2 N_b \left[1 + \frac{k''}{V_0^{1/3}} (c_l - c_l^s) \, t \right]^2 \qquad (8)$$

that is, the τ' vs. time curve will be quadratic in the early stages. However, this curve must tend to a limiting value, because $(c_l - c_l^s)$ becomes smaller with time due to the consumption of the reactant. Therefore, a sigmoid type of curve would be expected in this case, and has indeed been observed in many cases at low concentrations of surface active agents.

On the other hand, if $k''(c_l - c_l^s) \ll 1/W$, i.e. at surface active agent concentrations near the coagulation concentration, where the stability is low, equation (7) reads

$$\tau' = A_R V_0^2 N_b \left(1 + \frac{16 \pi \, \mathcal{D} \, N_b \, a_0}{W} \, t \right) \qquad (9)$$

This has the same form as the usual coagulation equation, cf. equation (4) of Part 2. This means that the coagulation process is predominant and the τ' vs. t curve assumes the usual form of a coagulation curve.

REFERENCES

(1) E. Matijević and R. H. Ottewill, *J. Colloid Sci.*, **13**, 242 (1958).

(2) R. W. Horne, E. Matijević, R. H. Ottewill and J. W. Weymouth, *Kolloid Z.*, **161**, 50 (1958).

(3) A. Watanabe, This Bulletin, **38**, 179 (1960).

(4) A. Watanabe, *ibid.*, **38**, 248 (1960).

(5) H. Reiss and V. K. La Mer, *J. Chem. Phys.*, **18**, 1 (1950).

(6) H. L. Frisch and F. C. Collins, *ibid.*, **20**, 1797 (1952).

(7) R. H. Doremus, *J. phys. Chem.*, **62**, 1968 (1958).